[논 문] 한국재료학회지
Korean J. Mater. Res.
Vol. 28, No. 6 (2018)

https://doi.org/10.3740/MRSK.2018.28.6.343

Mechanical Synthesis and Rapid Consolidation of Nanostructured W-Al_2O_3 Composite

BooRak Lee[1], GeolChae Jeong[1], GeunO Park[2] and In-Jin Shon[2†]

[1]Department of Advanced Materials Engineering,
Korea Polytechnic University, GyeongGi-Do, Republic of Korea
[2]Division of Advanced Materials Engineering, the Research Center of Hydrogen Fuel Cell,
Chonbuk National University, Jeonju, Jeonbuk 54896, Republic of Korea

(Received May 10, 2018 : Revised May 28, 2018 : Accepted May 28, 2018)

Abstract Recently, the properties of nanostructured materials as advanced engineering materials have received great attention. These properties include fracture toughness and a high degree of hardness. To hinder grain growth during sintering, it is necessary to fabricate nanostructured materials. In this respect, a high-frequency induction-heated sintering method has been presented as an effective technique for making nanostructured materials at a lower temperature in a very short heating period. Nanopowders of W and Al_2O_3 are synthesized from WO_3 and Al powders during high-energy ball milling. Highly dense nanostructured W-Al_2O_3 composites are made within three minutes by high-frequency induction-heated sintering method and materials are evaluated in terms of hardness, fracture toughness, and microstructure. The hardness and fracture toughness of the composite are 1364 kg/mm^2 and 7.1 MPa·m$^{1/2}$, respectively. Fracture toughness of nanostructured W-Al_2O_3 is higher than that of monolithic Al_2O_3. The hardness of this composite is higher than that of monolithic W.

Key words nanomaterial, sintering, composite, hardness, fracture toughness.

1. Introduction

Tungsten can potentially be an excellent high-temperature structural material because of its attractive properties e.g., a high melting point of 3,420 °C, an elastic modulus of 407 GPa, a hardness of 9.75 GPa, good thermal conductivity, a low coefficient of thermal expansion, and a low vapor pressure.[1)] However, it is difficult to achieve the sintering of a conventional microcrystalline W powder.[2,3)] Malewar et al.[4)] has reported that a sintered density as high as 97.4 % was achieved at 1,790 °C for 900 min, using nanopowder of W, but the grain size in this sintered W was remarkably coarse i.e., 15-30 μm, compared to an initial powder size of 8 nm.

Recently, the properties of nanostructured materials as advanced engineering materials have received great attention. These properties include fracture toughness and a high degree of hardness.[5,6)] To hinder the grain growth during sintering, it is necessary to fabricate nanostructured materials. In this respect, a high-frequency induction heated sintering method has been presented as an effective technique for making nanostructured materials at a lower temperature in a very short heating period.[7-9)] The grain growth of the W matrix is blocked by the presence of an oxide particle at the grain boundary of W. The dispersed oxide makes the enhancement of creep resistance and high-temperature strength due to pinning effect of grain boundary and block sliding of the grain boundary.[10)]

This study reports the fabrication of nanopowders of W and Al_2O_3 from WO_3 and 2 Al powders by a mechanical ball mill and nanostructured W-Al_2O_3 composites. These materials were made within three minutes by a high-frequency induction heated sintering method and evaluated in terms of its hardness, fracture toughness, and microstructure.

2. Experimental Procedures

Powders of WO_3(99.8 purity, < 10-20 μm, Alfa Aesar, Inc.) and Al(99.5 purity, < 45 μm, Alfa Aesar, Inc.) were

†Corresponding author
E-Mail : ijshon@chonbuk.ac.kr (I.-J. Shon, Chonbuk Nat'l Univ.)

used as initial materials. A high-energy ball mill (a Pulverisette-5 planetary mill) was conducted for 4 h under an argon atmosphere after WO_3 and 2Al powders were mixed. WC-8Co hard materials were used as balls with 10 mm in diameter.

Milled powder(Al_2O_3-W) was placed in a graphite die using upper and lower graphite punches. High-frequency induction heated sintering equipment is shown schematically in Ref.[11] The sintering process consists of four stages. In stage 1, the system was evacuated under a vacuum of 20 Pa. A uniaxial pressure of 80 MPa was applied to powder in stage 2. An induced current was introduced and maintained to 1,400 °C with a heating rate of 1,000 °C/minute in stage 3. And then the powder was turned off without holding time. The specimen was cooled to room temperature at the end of the stage.

Grain sizes of W and Al_2O_3 were calculated by Suryanarayana and Grant Norton's equation.[12] Relative densities of the sintered specimen were evaluated after calculating the volume of the sample using Archimedes' method. Microstructure information of W-Al_2O_3 composite was observed using SEM with EDS. Phases were evaluated using X-ray diffraction(XRD). Vickers hardness and fracture toughness were calculated, using indentations and crack length on the sintered specimen at a load of 196 N.

3. Results and Discussion

Fig. 1 displays X-ray diffraction patterns of initial powders. In Fig. 1(a) and (b), all peaks are WO_3 and Al, respectively. XRD pattern of ball milled powders is shown in Fig. 2. Here reactant peaks of WO_3 and Al were not observed. Instead, product peaks of W and Al_2O_3 were detected. In Fig. 2, full width at half-maximum of the diffraction peak is broad. This indicates that strain was introduced, and powders were refined during the milling. Reactant powders milled with high-energy balls were synthesized during the milling according to equation (1).

$$WO_3 + 2\ Al \rightarrow W + Al_2O_3 \quad (1)$$

The interaction between WO_3 and 2 Al in equation (1) is thermodynamically feasible as shown in Fig. 3. Fig. 4 displays a plot of $B_r \cos\theta$ versus $\sin\theta$ to calculate powder sizes of W and Al_2O_3 by Suryanarayana and Norton's formula.[12] Powder sizes of W and Al_2O_3 were 28 and 40 nm, respectively. FE-SEM image and EDS of W-Al_2O_3 powder milled for 4 hours are shown in Fig. 5. Milled powders consist of nanopowders with some agglomeration. In EDS, only W, Al and O peaks were detected without other peaks such as WC and Co, which is possible to introduce during the ball milling.

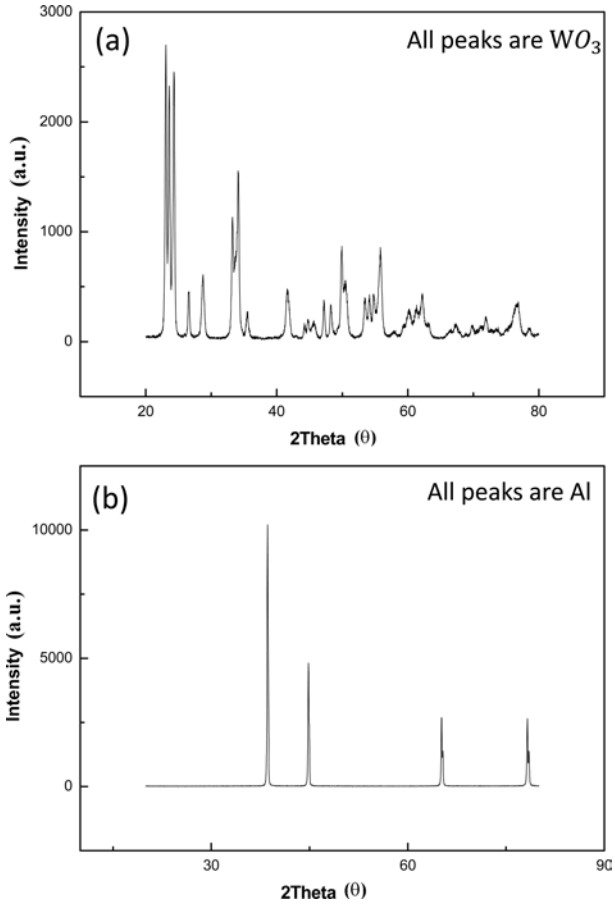

Fig. 1. XRD patterns of raw powders : (a) WO_3 powder, (b) Al powder.

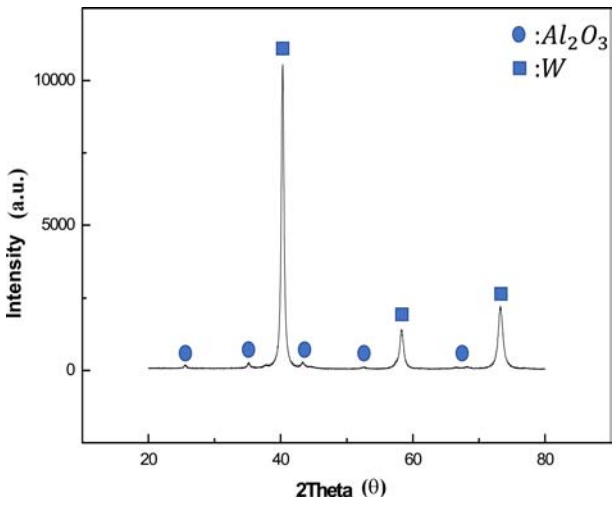

Fig. 2. X-ray diffraction patterns of Al_2O_3+W powder milled by high energy ball milling for 4 hours.

Fig. 6 displays variation of shrinkage displacement and temperature with heating time during sintering of W-

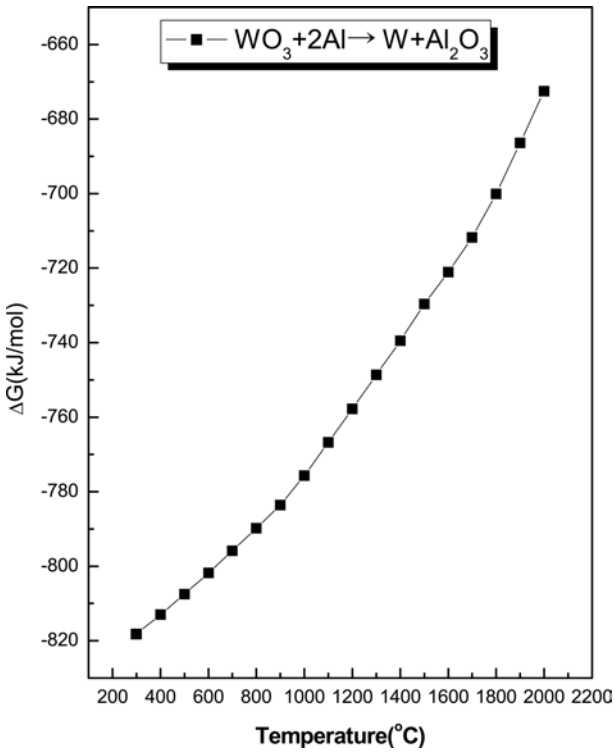

Fig. 3. The Gibbs free energy variation with temperature by interaction of WO_3 with 2 Al.

Al_2O_3 composite. Thermal expansion shows up to 900 °C as the induced current was applied. And then shrinkage displacement abruptly increased up to 1,200 °C. Shrinkage displacement is nearly constant above the temperature. This means that nearly full density is achieved at 1,400 °C. Fig. 7 displays X-ray diffraction pattern of W-Al_2O_3 composite heated to 1,400 °C, in which only W and Al_2O_3 peaks were detected. The corresponding relative density of this composite was 98 %.

The plots of sinθ versus B_r cosθ to calculate grain size of W and Al_2O_3 are displayed in Fig. 8. Average grain sizes of W and Al_2O_3 in the composite are 148 and 55 nm, respectively. R. Malewar[4] has reported that a sintered

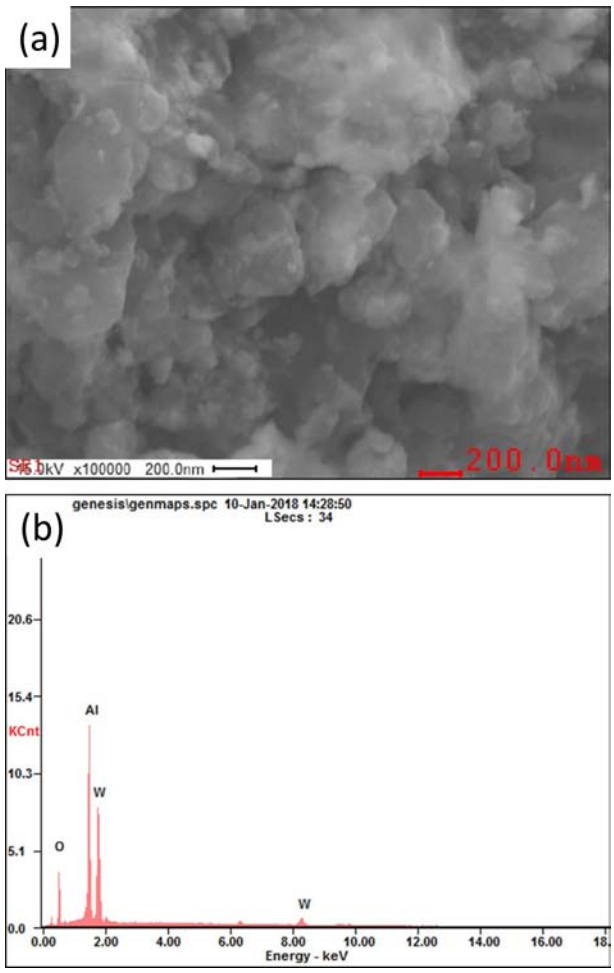

Fig. 5. (a) FE-SEM image and (b) EDS analysis of W+ Al_2O_3 powder milled for 4h.

density as high as 97.4 % was achieved at 1,790 °C for 900 min using nanopowder of W milled by a high-energy ball mill, but the grain size of this sintered W was remarkably coarse as 15-30 μm, compared to initial powder size of 8 nm. In our study, dense nanostructured W- Al_2O_3 was achieved in 1,400 °C and 3 min using

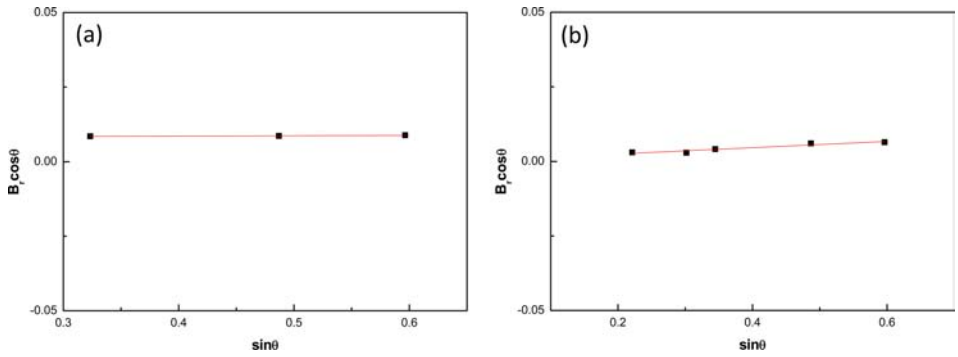

Fig. 4. Plot of B_r cosθ versus sinθ for W and Al_2O_3 powder milled for 4h.

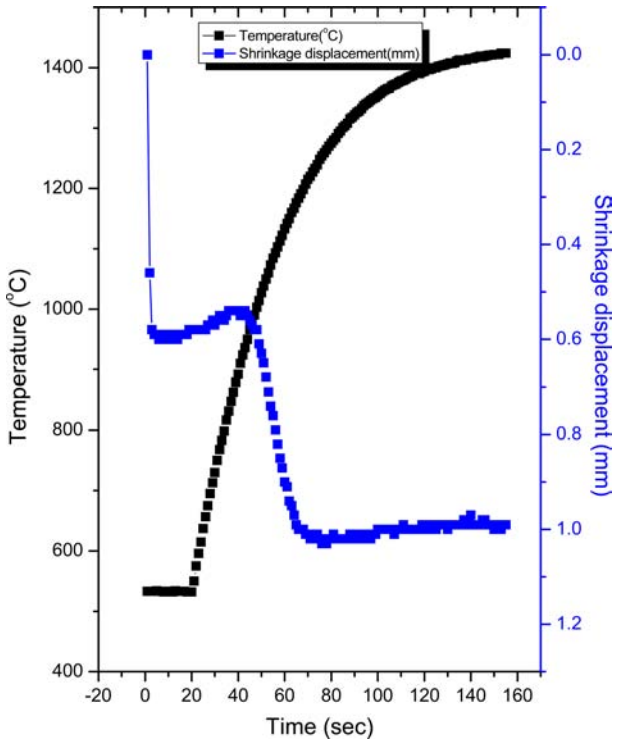

Fig. 6. Variations of temperature and shrinkage displacement with heating time during the sintering of W-Al_2O_3 powder.

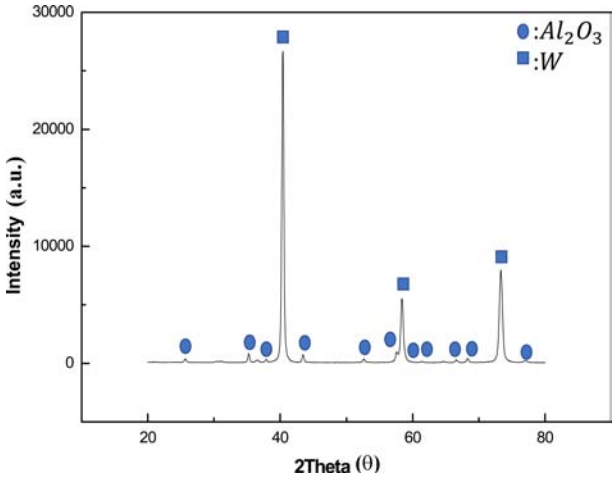

Fig. 7. X-ray diffraction patterns of Al_2O_3+W composite sintered using high-frequency induction heating.

nanopowder of W and Al_2O_3 milled by high-energy ball mill. And nanostructured W- Al_2O_3 composite was obtained in a shorter time and lower temperature. Reasons for highly dense nanostructured composite obtained within three minutes at low temperature are as follows. Three factors that contribute to rapid consolidation process can be explained. First, electrical field generated spark discharges that cleaned the surface of powders. Grain

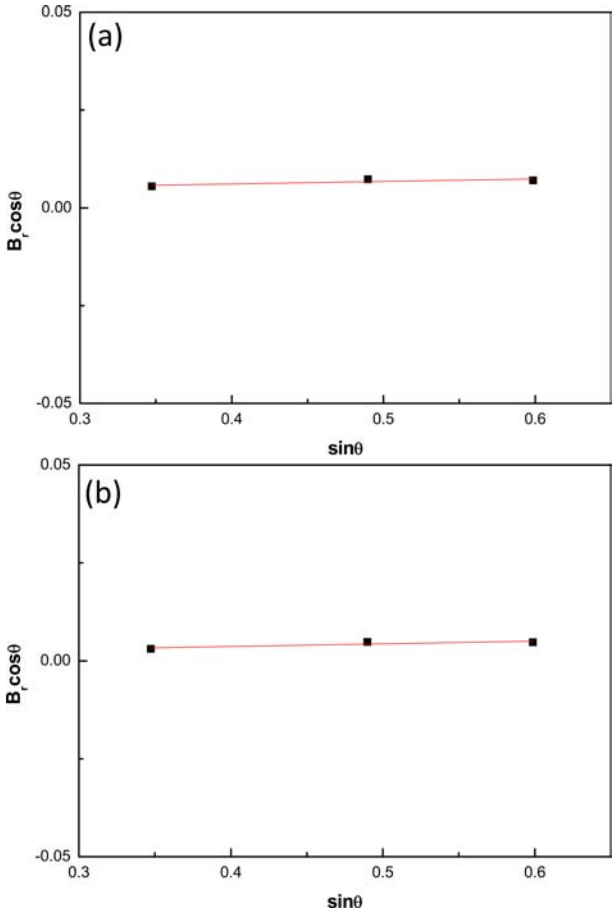

Fig. 8. Plot of $B_r \cos\theta$ versus sinθ for W (a) and Al_2O_3 (b) in the composite sintered at 1,400 °C.

boundary diffusion can increase due to this cleaning. Atomic diffusion can enhance under the electric field due to electromigration.[13,14] Second, application of pressure during the sintering is helpful in removing pores in the specimen and increasing driving force. Third, high-energy ball mill produced defect, strain and finer powder facilitating sintering.[15,16] So, the sintering temperature of milled powders is lower than that of un-milled powders.[17]

Fig. 9 displays FE-SEM image and X-ray mapping of the sample sintered at 1,400 °C. Microstructure consists of ultra-fine grey phase and bright phase. Grey and bright phase in Fig. 9 are Al_2O_3 and W, respectively from mass contrast and X-ray mapping.

Vickers hardness was evaluated on polished sections of the W-Al_2O_3 composite under a 196 N load. The calculated hardness value of W-Al_2O_3 composite sintered at 1,400 °C was 1,364 kg/mm^2. This value is higher than that of monolithic W reported as 9.75 GPa.[1] Cracks propagated from indent corners as shown in Fig. 10(a). Length of these cracks can permit fracture toughness using the Niihara's equation.[18] Fracture toughness value of the W-Al_2O_3 composite measured by this method is

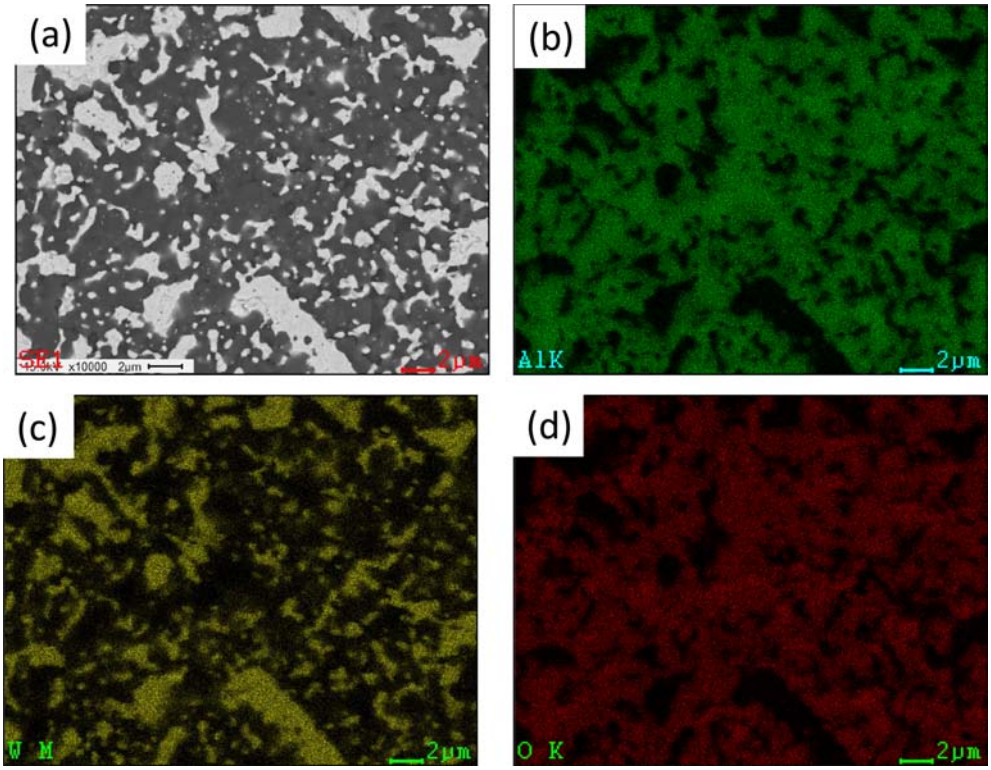

Fig. 9. FE-SEM image and EDS analysis of W-Al_2O_3 composite : (a) FE-SEM image, (b) Al mapping, (c) W mapping, (d) O mapping.

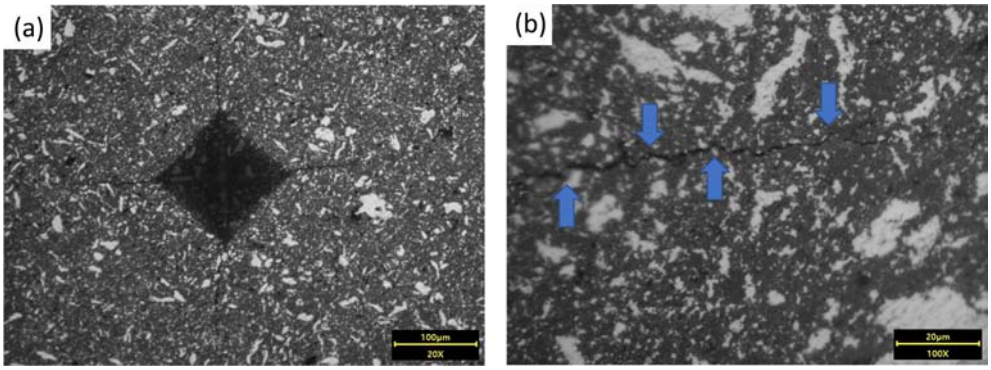

Fig. 10. (a) Vickers hardness indent and (b) crack propagating in W-Al_2O_3 composite.

7.1 MPa·$m^{1/2}$. Fracture toughness of the W-Al_2O_3 composite is higher than that of monolithic Al_2O_3 reported as 4 MPa·$m^{1/2}$.[19] A crack propagated in a branching(↑) and deflective manner(↓) in Fig. 10(b). Enhanced fracture toughness of W-Al_2O_3 composite is believed that W and Al_2O_3 in the composite may deter propagation of cracks and W and Al_2O_3 have nanostructured phases.

4. Conclusions

Nanopowders of W and Al_2O_3 were synthesized during the high-energy ball mill from WO_3 and 2Al powders. The nanostructured W-Al_2O_3 composite was achieved within three minutes from synthesized powder by high-frequency induction heated sintering. Average grain sizes of W and Al_2O_3 in composite sintered at 1,400 °C are 148 and 55 nm, respectively and the relative density of the composite was 98 %. The hardness and fracture toughness of the composite was 1,364 kg/mm^2, 7.1 MPa·$m^{1/2}$, respectively. Fracture toughness of the W-Al_2O_3 composite is higher than that of monolithic Al_2O_3 reported as 4 MPa·$m^{1/2}$. Enhanced fracture toughness of W-Al_2O_3 composite is believed that W and Al_2O_3 in the composite may deter propagation of cracks and W and Al_2O_3 have

nanostructured phases.

Acknowledgment

This research was supported by Basic Science Research Program though the National Research Foundation of Korea(NRF) funded by the Ministry of Education (2015R1D1A1A01056600) and this work was supported by the Korea Institute of Energy Technology Evaluation and Planning(KETEP) and the Ministry of Trade, Industry & Energy(MOTIE) of the Republic of Korea(No. 20184-030202210).

References

1. W. F. Smith, Structure and Properties of Engineering Alloys, 2nd ed., p.580, McGraw Hill, New York, U.S.A. (1993).
2. L. Uray, Int. J. Refract. Met. Hard Mater., **20**, 311 (2002).
3. L. Uray, Int. J. Refract. Met. Hard Mater., **20**, 319 (2002).
4. R. Malewar, K. S. Kumar, B. S. Murty, B. Sarma, and S. K. Pabi, J. Mater. Res., **22**, 1200 (2007).
5. M. Sherif El-Eskandarany, J. Alloys Compd., **305**, 225 (2000).
6. I.-J. Shon, Int. J. Refract. Met. Hard Mater., **64**, 242 (2017).
7. I.-J. Shon and S.-J. Lee, Int. J. Refract. Met. Hard Mater., **65**, 69 (2017).
8. I.-J. Shon, Korean J. Met. Mater., **54**, 826 (2016).
9. I.-J. Shon, Int. J. Refract. Met. Hard Mater., **72**, 257 (2018).
10. E. Lassner and W-D. Schubert, Tungsten-properties, chemistry, technology of the element, alloys, and chemical compounds, Kluwer Academic/Plenum Publishers, New York, 1999, pp. 255.
11. I.-J. Shon, H. J. Kwon, and H.-S. Oh, Electron. Mater. Lett., **10**, 337 (2014).
12. C. Suryanarayana and M. Grant Norton, X-ray diffraction: a practical approach, Plenum Press, New York, 1998.
13. Z. Shen, M. Johnsson, Z. Zhao, and M. Nygren, J. Am. Ceram. Soc., **85**, 1921 (2002).
14. J. E. Garay, U. Anselmi-Tamburini, Z. A. Munir, S. C. Glade, and P. Asoka-Kumar, Appl. Phys. Lett., **85**, 573 (2004).
15. I.-J. Shon, Ceram. Int., **42**, 15113 (2016).
16. I.-J. Shon, Ceram. Int., **42**, 13314 (2016).
17. W. B. Kim, K.-M. Roh, J.-W. Lim, H.-S. Oh, and I.-J. Shon, J. Alloys Compd., **574**, 260 (2013).
18. K. Niihara, R. Morena, and D. P. H. Hasselman, Mater. Sci. Lett., **1**, 13 (1982).
19. M. N. Rahaman, A. Yao, B. S. Bal, J. P. Garino, and M. D. Ries, J. Am. Ceram. Soc., **90**, 1965 (2007).